How to cite: *Angew. Chem. Int. Ed.* **2022,** *61,* e202201684
International Edition: doi.org/10.1002/anie.202201684
German Edition: doi.org/10.1002/ange.202201684

Antiviral Agents

Harnessing Natural Products by a Pharmacophore-Oriented Semisynthesis Approach for the Discovery of Potential Anti-SARS-CoV-2 Agents

Yuan-Fei Zhou[+], Bing-Chao Yan[+], Qian Yang[+], Xin-Yan Long[+], Dan-Qi Zhang, Rong-Hua Luo, Han-Yu Wang, Han-Dong Sun, Xiao-Song Xue, Yong-Tang Zheng,* and Pema-Tenzin Puno**

Abstract: Natural products possessing unique scaffolds may have antiviral activity but their complex structures hinder facile synthesis. A pharmacophore-oriented semisynthesis approach was applied to (−)-maoelactone A (**1**) and oridonin (**2**) for the discovery of anti-SARS-CoV-2 agents. The Wolff rearrangement/lactonization cascade (WRLC) reaction was developed to construct the unprecedented maoelactone-type scaffold during semisynthesis of **1**. Further mechanistic study suggested a concerted mechanism for Wolff rearrangement and a water-assisted stepwise process for lactonization. The WRLC reaction then enabled the creation of a novel family by assembly of the maoelactone-type scaffold and the pharmacophore of **2**, whereby one derivative inhibited SARS-CoV-2 replication in HPA EpiC cells with a low EC_{50} value (19 ± 1 nM) and a high TI value (>1000), both values better than those of remdesivir.

[*] Dr. Y.-F. Zhou,[+] Dr. B.-C. Yan,[+] Dr. Q. Yang,[+] H.-Y. Wang, Prof. Dr. H.-D. Sun, Prof. Dr. P.-T. Puno
State Key Laboratory of Phytochemistry and Plant Resources in West China, and Yunnan Key Laboratory of Natural Medicinal Chemistry
Kunming Institute of Botany, University of Chinese Academy of Sciences, Chinese Academy of Sciences
Kunming 650201 (China)
E-mail: punopematenzin@mail.kib.ac.cn

X.-Y. Long,[+] Dr. R.-H. Luo, Prof. Dr. Y.-T. Zheng
Key Laboratory of Animal Models and Human Disease Mechanisms of the Chinese Academy of Sciences, Kunming Institute of Zoology, Chinese Academy of Sciences
Kunming 650223 (China)
E-mail: zhengyt@mail.kiz.ac.cn

D.-Q. Zhang, Prof. Dr. X.-S. Xue
State Key Laboratory of Elemento-organic Chemistry, College of Chemistry, Nankai University
Tianjin 300071 (China)
and
Key Laboratory of Organofluorine Chemistry, Shanghai Institute of Organic Chemistry, University of Chinese Academy of Sciences, Chinese Academy of Sciences
345 Lingling Road, Shanghai 200032 (China)
E-mail: xuexs@sioc.ac.cn

[+] These authors contributed equally to this work.

Introduction

The COVID-19 pandemic caused by severe acute respiratory syndrome coronavirus 2 (SARS-CoV-2) has had an enormous impact on human life and production. According to statistics (https://coronavirus.jhu.edu/map.html), more than 370 million people have been infected and 5.6 million people have died. Vaccine defense is currently the main method employed against SARS-CoV-2, but drug intervention is still urgently needed. SARS-CoV-2 encodes 4 structural proteins and 16 nonstructural proteins (NSPs),[1] providing multiple targets for potential drugs. SARS-CoV-2 $3CL^{pro}$ is an essential cysteine protease among these NSPs that is present during the viral life cycle, and the absence of any closely related homologs in human cells makes this NSP an attractive drug target.[2] Researchers have been studying active molecules for use against SARS-CoV-2 $3CL^{pro}$. Nirmatrelvir (a drug in Paxlovid)[3] and other promising covalent inhibitors, including Michael acceptors,[4] α-ketoamides,[5] aldehydes,[6] and Re complexes[7] have been reported. Natural products (NPs) are derived from organisms in nature, and the impact and continuing role of NPs in promoting drug discovery cannot be overemphasized. Therefore, the discovery of covalent molecules derived from NPs for use against SARS-CoV-2 $3CL^{pro}$ and SARS-CoV-2 remains promising.

Structural complexity prevents the facile synthesis of NPs, which are usually not available in sufficient quantities from natural sources for further development. Therefore, chemists have adopted synthetic strategies to incorporate rich information on collections of NPs into synthetic research to discover drugs in an economical and time-efficient manner.[8] Here, we describe a pharmacophore-oriented semisynthesis (POSS) approach to integrate natural scaffolds into biological studies (Figure 1a). The proposed approach utilizes a pharmacophore from framework A (a commercial source or plants with a high content of the pharmacophore) and a biogenetically relevant novel natural scaffold from framework B to form a new combination to facilitate drug discovery.

Herein, we demonstrate the application of POSS to two *ent*-kaurane diterpene members in a chemical synthesis to create lead compounds for anti-SARS-CoV-2 agents. One member is (−)-maoelactone A (**1**), which possesses an

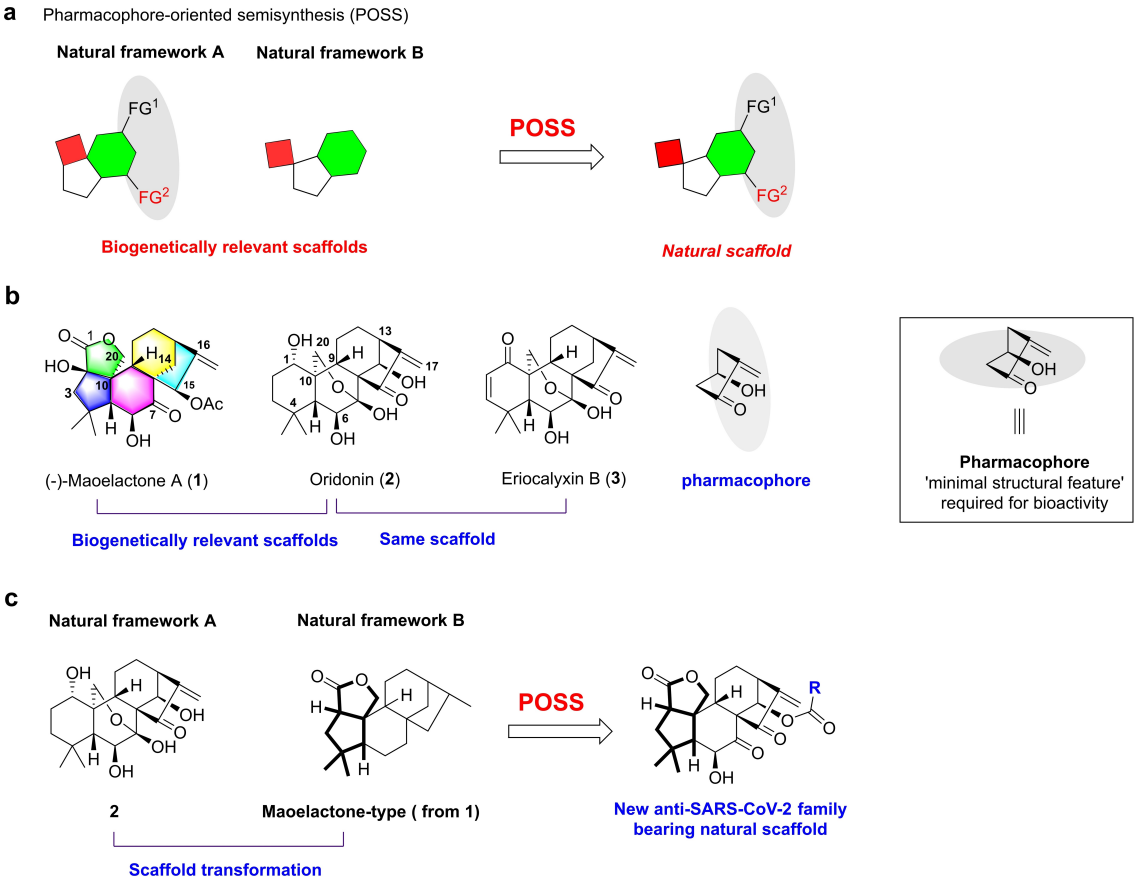

Figure 1. Pharmacophore-oriented semisynthesis (POSS) approach and speculation on its application to (−)-maoelactone A (**1**) and oridonin (**2**). a) POSS seeks to align natural scaffolds with biological studies. b) **1** bearing an unprecedented maoelactone-type scaffold and **2** featuring the pharmacophore. c) Assembly maoelactone-type scaffold with the pharmacophore by scaffold transformation, leading to discovery of a novel anti-SARS-CoV-2 family.

unprecedented maoelactone-type scaffold from *Isodon eriocalyx*, and the other member is oridonin (**2**),[9] which carries a pharmcophore and is both a commercial product and present in a high content in *I.* rubescens. A Wolff rearrangement/lactonization cascade (WRLC) reaction was developed for the construction of the maoelactone-type scaffold during semisynthesis of **1**, enabling the creation of a novel anti-SARS-CoV-2 family from **2** by assembly of the pharmacophore with the maoelactone-type scaffold and leading to the discovery of potential anti-SARS-CoV-2 agents. Compound **70** inhibited SARS-CoV-2 replication in HPA EpiC cells with a low EC_{50} value (19 ± 1 nM) and a high TI value (> 1000), both values better than those of remdesivir.

Results and Discussion

An α,β-unsaturated ketone group and a 14-hydroxyl group were selected as the pharmacophore for **2** based on several lines of evidence (Figure 1b).[10] A collection of NP libraries was previously screened to identify inhibitors of SARS-CoV-2, and several natural products containing α,β-unsaturated ketones were found to perform well: oridonin possessed an EC_{50} of 1.46 μM for SARS-CoV-2 (where chloroquine with an EC_{50} of 1.78 μM was used as a positive control)[11] but a low TI value (>40). Recent research also indicated **2** bound covalently to the SARS-CoV-2 replicase Nsp9 and SARS-CoV-2 $3CL^{pro}$.[12] Furthermore, compound **1** (0.7 mg from 25 kg of plant material) was firstly isolated as a rearranged diterpenoid with an unprecedented 1,10-*seco*-2,10-*abeo*-1,20-lactone scaffold using nuclear magnetic resonance and mass spectrometry (for a detailed analysis, see Supporting Information, Figure S1). We envisioned that the unprecedented scaffold of **1** may improve the bioactivity of **2** based on several examples of modification in the ring A increasing the biological effects.[13] We named this scaffold maoelactone-type, although the absolute configuration of the scaffold, including C-2 and C-10, remains to be determined. Therefore, a semisynthesis of **1** from eriocalyxin B (**3**)[14] could be conducted to provide the stereochemistry of the maoelactone-type scaffold, and a straightforward synthetic method could be developed to construct the maoelactone-type scaffold as a scaffold-transformation approach for **2**. The direct synthetic approach could be further applied to establish a novel anti-SARS-CoV-2 family by combining the pharmacophore of **2** with a maoelactone-type scaffold, thereby harvesting the full potential of the maoelactone scaffold (Figure 1c).

The synthetic route of **1** was proposed from **3** (Scheme 1a), in which **3** underwent sequential reduction reactions at the C-15 carbonyl and double bond between C-2 and C-3. Further carbene formation at C-2 could enable the transformation of **5** to **8** via a challenging rearrangement and lactone formation. Finally, **8** underwent oxidation at the C-2 position and acetylation at C-15 to form **1**. Hence, compound **3** was used as a starting material and we had kilograms of the sample on hand. Our synthesis started with the protection of HO-6 with the SEM group, and subsequent hydrogenation by $NaBH_4$ at −50 °C in THF transformed the C-15 ketone to a β-oriented hydroxyl group of **11**,[15] the structure of which was confirmed by single X-ray crystal diffraction.[16] A reduction system of $NiCl_2{\cdot}6H_2O/NaBH_4$[17] saturated the double bond of α,β-unsaturated carbonyl between C-2 and C-3 to produce compound **12** in 76 % yield. To construct a carbene precursor, the α-diazoketone **13** was prepared in the presence of tosyl azide and DBU, and the stereochemistry of **13** was confirmed by single X-ray crystal diffraction analysis[16] (Scheme 1b). With a large quantity of **13** in hand, we initially used UV at 300 nm to render the expected 5/5-fused bicyclic lactone (**14**) in 83 % yield. We further investigated the temperature and illuminating sources to determine optimal synthesis conditions (Scheme 2a). Both the heating temperature and light source considerably influenced the yield. After many attempts, we identified the optimal conditions (toluene, 110 °C, 2 hours) under which **13** could produce **14** in 90 % yield (entry 6). To the best of our

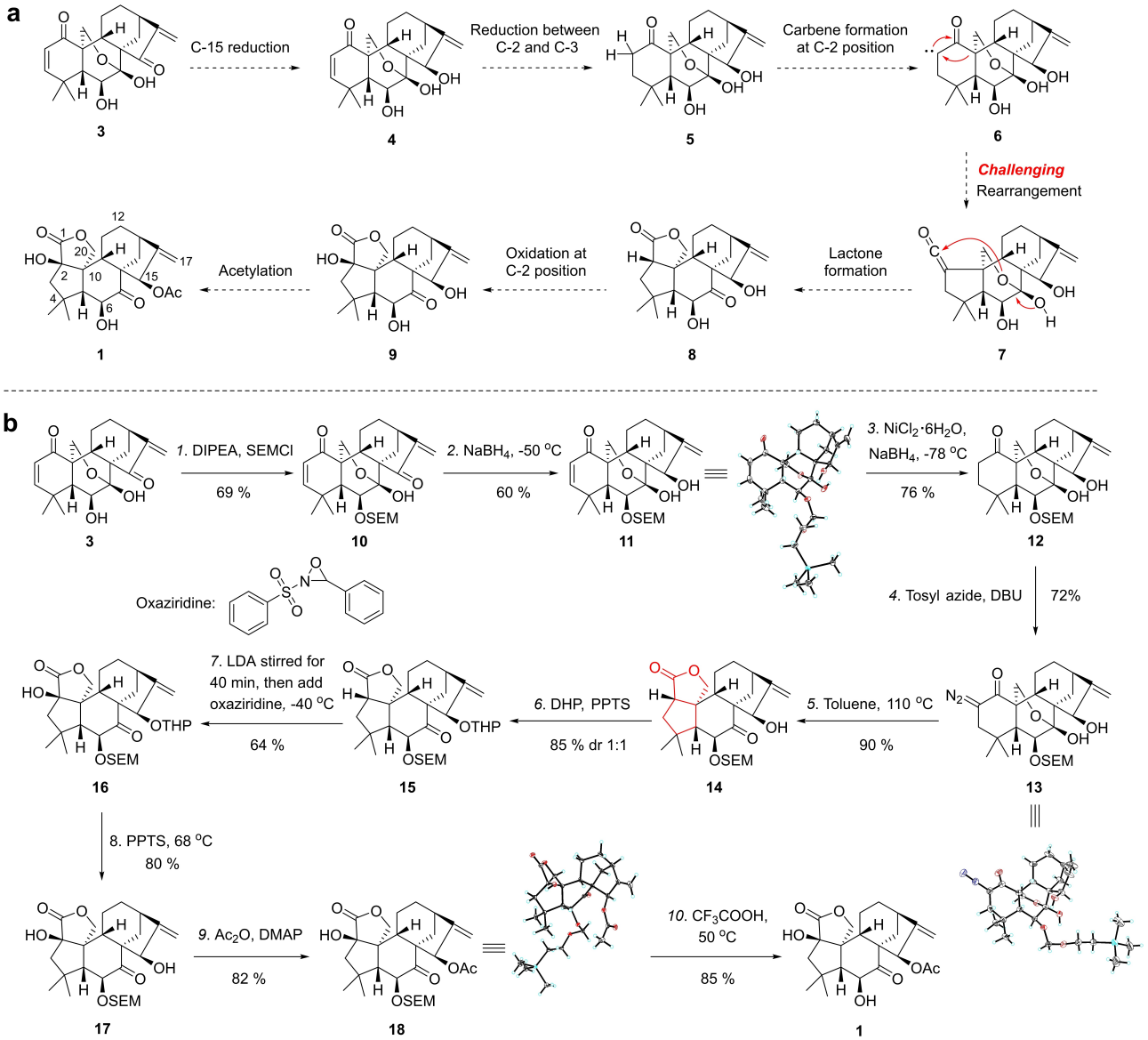

Scheme 1. Proposed synthetic route and semisynthesis of (−)-maoelactone A (**1**). a) Proposed synthetic route of **1** from **3**. b) Semisynthesis of **1** from **3** confirmed stereochemistry of maoelactone-type scaffold and provided Wolff rearrangement/lactonization cascade (WRLC) reaction for applying the POSS approach. DIPEA = *N*,*N*-diisopropyl-ethylamine, SEMCl = 2-(trimethylsilyl)-ethoxymethyl chloride, DBU = 1,8- diazabicyclo-[5.4.0]undec-7-ene, DHP = 3,4-dihydro-2*H*-pyran, THP = tetrahydropyran, PPTS = pyridinium p-toluenesulfonate, LDA = lithium diisopropylamide, Ac_2O = acetic anhydride, DMAP = 4-dimethylaminopyridine.

a

13 14

Entry	T [°C]	Light	Solvent	Time [h]	Yield [%][a]
1	40	/	CH_2Cl_2	24	trace
2	66	/	THF	24	27
3	81	/	MeCN	12	62
4	80	/	toluene	6	65
5	100	/	toluene	4	86
6	110	/	toluene	2	90
7	110	/	neat	2	76
8	25	313 nm[b]	toluene	2	83
9	25	blue LED[c]	toluene	24	82
10	25	HPSL[c]	toluene	1	trace
11	25	HPML[c]	toluene	1	88
12	25	HPML[c]	neat	1	43

Note: [a] Isolated yield after flash chromatography. [b] Photoreactor with 16×60W mercury lamps. [c] Abbreviations: blue LED, blue light emitting diode; HPSL, high pressure sodium lamp; HPML, high pressure mercury lamp.

b

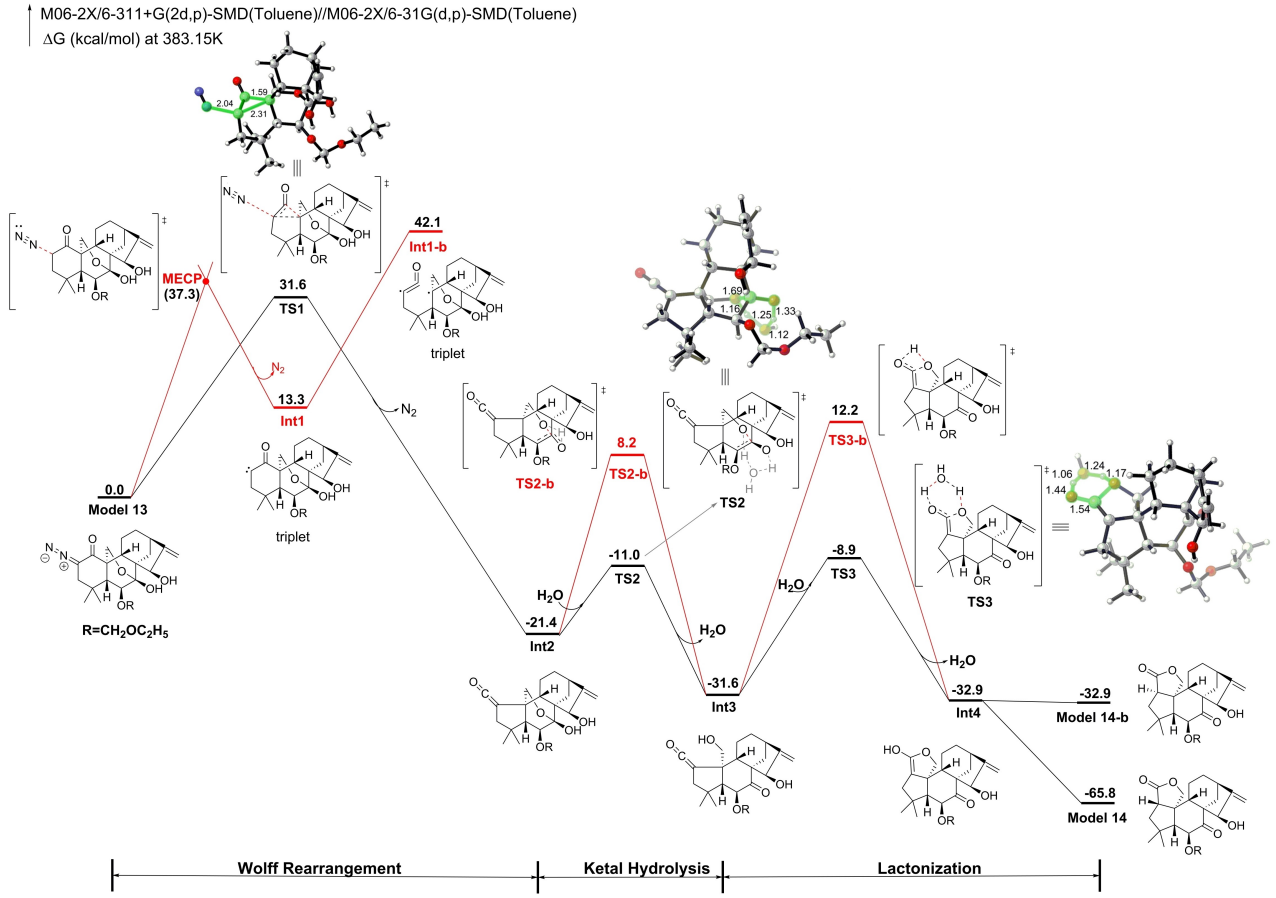

Scheme 2. Optimization and mechanistic study of Wolff rearrangement/lactonization cascade (WRLC) reaction. a) Conditional optimization for WRLC reaction. b) Mechanistic study of WRLC reaction at the M06-2X/6-311+G(2d,p)-SMD(Toluene)//M06-2X/6-31G(d,p)-SMD(Toluene) level.

knowledge, this report is the first use of an intramolecular Wolff rearrangement/lactonization cascade (WRLC) reaction for a hemiketal/α-diazoketone system to directly assemble 3-oxabicyclo[3.3.0]octan-2-one motif (maoelactone-type scaffold) in one step. To elucidate the mechanism of the WRLC reaction, DFT calculations were performed at the M06-2X/6-311+G(2d,p)- SMD//M06-2X/6-31G(d,p)-SMD level of theory, where a simplified substrate was used to investigate a model reaction (Scheme 2b) (see Supporting Information for computational details). The calculation results reveal that a concerted nitrogen extrusion and 1,2-shift mechanism is preferred over a stepwise mechanism involving a carbene intermediate for the Wolff rearrangement. The resulting ketene intermediate subsequently undergoes facile water-assisted ketal hydrolysis and lactonization to produce the 5/5-fused bicyclic lactone (example for water acting as a catalyst in "anhydrous" reaction[18]). The anti-5/5-fused bicyclic lactone is predicted to be more stable than the syn product by ca. 33 kcal mol^{-1} (Scheme 2b). This result is consistent with the experimental observation that

anti-5/5-fused bicyclic lactone was the sole lactone product. The WRLC reaction realizes an important scaffold transformation and therefore overcomes the most difficult problem in the implementation of the POSS approach. With **14** in hand, we directed our attention to the hydroxylation of C-2 position. Initial attempts at direct hydroxylation of **14** at C-2 led to a retro-aldol process under basic conditions, even in triethylamine. The other option was to first acetylate the C-15 position and then install a hydroxyl group at the C-2 position. In fact, enolate formation from the acetyl group followed by reaction with the C-7 carbonyl group[19] afforded the "cage"-like motif of **S3** with crystal evidence[16] (Figure S4). Protection and deprotection of the 15-hydroxyl group with DHP under acidic conditions were screened for compatibility with hydroxylation at the C-2 position. The obtained **15a** and **15b** (85 %, dr 1:1) were then subjected to stereoselective hydroxylation (LDA/Davis reagent[20]), furnishing **16a** and **16b** in 64 % yield, which were then subjected to selective deprotection and acetylation. Single-crystal X-ray diffraction of **18** with a fine Flack parameter (0.008)[16] confirmed the β-orientation of C-2 and configuration of C-10. Finally, removal of SEM with TFA delivered (−)-maoelactone A (**1**) in 85 % yield. The spectroscopic data of synthetic **1** matched those of the natural isolate (Table S1, Figures S2 and S3), establishing the stereochemistry as 2*R*,5*R*,6*S*,8*S*,9*S*,10*S*,13*R*,15*R*. This semisynthesis unambiguously verified the stereochemistry of the novel maoelactone-type scaffold. More importantly, the newly developed WRLC reaction enabled the installation of maoelactone-type scaffolds during synthesis, providing tools for applying the POSS approach.

Oridonin (**2**) is a single drug component that is currently in a clinical observational study (http://www.chictr.org.cn/enIndex.aspx; ChiCTR-OOB-16007883), and phase I clinical trials are being conducted in China on its derivative HAO-472 to treat acute myeloid leukemia (www.chinadrugtrials.org.cn; CTR20150246). In the early stage of synthetic planning, we utilized **3** to construct a maoelactone-type scaffold, mainly considering that **3** had the same scaffold as **2**. As our aim was to assemble the pharmacophore of **2** and maoelactone-type scaffold together, we needed to determine whether the WRLC reaction could be applied to **2** without changing the pharmacophore. As shown in Scheme 3a, treatment of **2** with Jones reagent in acetone provided **19** in 80 % yield, which further underwent reduction of $NaBH(OAc)_3$ and AcOH to readily produce **20** in 78 % yield. Compound **20** was treated with TMSCl and DIPEA in DCM, reacted with DBU and TsN_3 in CH_3CN and finally TMS was removed using TBAF to afford **21**. Treatment of **21** with DMP and $NaHCO_3$ at 0 °C produced **22**. A subsequent key WRLC reaction transformed **22** into the product **23** in 81 % yield at the gram scale and successfully combined the pharmacophore with a maoelactone-type scaffold in one step. After completing the synthesis of **23**, we continued to create a novel scaffold family by introducing different types of substituents, including alkyl, aryl and heterocyclic substituted esters at the 14-OH position. Family members **24**–**86** were synthesized (Scheme 3b) that shared the same natural maoelactone-type scaffold.

Family members **23**–**86** together with **1** and **2** at a concentration of 5 μM were investigated for use against SARS-CoV-2 $3CL^{Pro}$. As shown in Figure 2a, most of the covalent inhibitors were able to inhibit enzymatic activities, with inhibition rates ranging from 10 % to 99 % (Figure 2a). Compounds with high inhibition rates contained bromine (**47**, **57**, and **63**) and 2-haloisonicotine (**53**, **55**, and **57**). Simple structural units (**30**, **31**, **35**, **39**, **40**, and **41**) appeared to be more active than large complex substituents and compound **2**. The IC_{50} values of the compounds exhibiting inhibition rates of over 80 % were quantified (Figure 2b). The IC_{50} values of the derivatives ranged between 0.463 and 2.427 μM, of which **35** and **47** showed the highest efficacy against SARS-CoV-2 $3CL^{Pro}$ with IC_{50} values of 0.463 and 0.477 μM, respectively. A possible binding site was the Cys145 residue[12b] and covalent docking result indicated that **70** binded well into the binding pocket of SARS-CoV-2 $3CL^{pro}$ and formed a covalent bond with Cys145 (see Supporting Information, Figure S5). Besides, to a certain extent, the type of compounds exhibited selectivity against some cysteine proteases, including Cathepsin B and Caspase-1 (see Supporting Information, Figure S6). The compounds with excellent efficacy against SARS-CoV-2 $3CL^{Pro}$ were subjected to viral load testing by quantitative reverse-transcription polymerase chain reaction (RT-qPCR) analysis. Vero E6 and HPA EpiC cells were infected with SARS-CoV-2 and treated with different concentrations of the test compounds. The RT-qPCR results revealed that all nine compounds, including **2**, inhibited SARS-CoV-2 virus replication in HPA EpiC cells with EC_{50} values ranging from 19 nM to 7.78 μM and in Vero E6 cells with EC_{50} values ranging from 20 nM to 2.07 μM. Most of the test compounds (**31**, **35**, **47**, **53**, **55**, and **70**) exhibited higher activities and TIs in both SARS-CoV-2-affected Vero E6 and HPA EpiC cells than **2** (Figure 2c). Compound **55** exhibited excellent activity with a low EC_{50} value (20 ± 7 nM) in Vero E6 cells but had a relatively low TI (523.81–555.41) because of cytotoxicity. However, compound **70** inhibited SARS-CoV-2 virus replication in HPA Epic cells with low EC_{50} values (19 ± 1 nM) and high TI values (>1000), where both sets of values were better than those of the positive control remdesivir.

Conclusion

As it is believed that SARS-CoV-2 will be a part of human life over the next few years,[21] more small-molecule drugs need to be developed and reserved for the current and future (as yet unknown) viruses. NPs remain essential for the discovery of small molecules with unique biological activities. The *ent*-kaurane diterpenoids are a large class of NPs with more than 1200 members, and their isolation, structural elucidation, chemical synthesis, and biological evaluation have attracted considerable attention.[22] Many complex *ent*-kaurane family members with excellent bioactivity, including maoecystal V,[23] jungermatrobrunin A,[24] jungermannenones B and C,[25] glaucocalyxin A,[26] farnesin,[27] and the shikoccin family,[28] have been developed to construct target molecules by total synthesis. However,

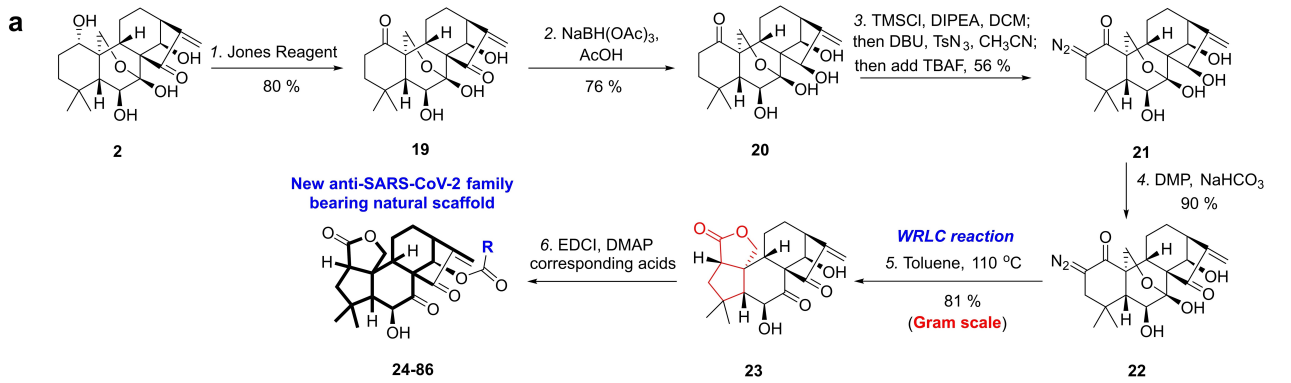

b

NO.	R	NO.	R	NO.	R	NO.	R	NO.	R	NO.	R	NO.	R
24		33		42		51	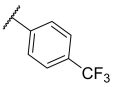	60	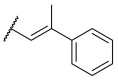	69	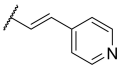	78	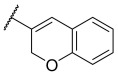
25		34		43		52		61	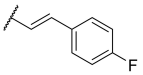	70	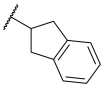	79	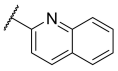
26	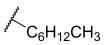	35		44		53	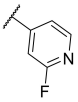	62	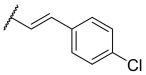	71	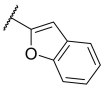	80	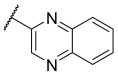
27	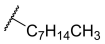	36		45	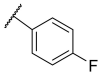	54		63	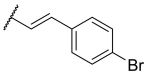	72	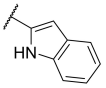	81	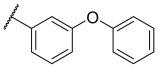
28		37		46	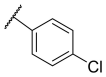	55	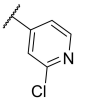	64	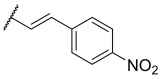	73	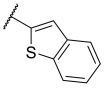	82	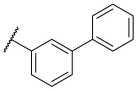
29		38		47	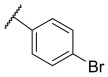	56		65		74		83	
30		39		48		57		66		75		84	
31		40		49		58		67		76		85	
32		41		50		59		68		77		86	

Scheme 3. Assembly the pharmacophore of oridonin (**2**) with the maoelactone-type scaffold by WRLC reaction to create a novel family. a) Steps to combine the pharmacophore of **2** with maoelactone-type scaffold by WRLC Reaction. b) Chemical structures of family members **24**–**86**. TMSCl = chlorotrimethylsilane, TsN_3 = tosyl azide, DMAP = 4-dimethylaminopyridine, TBAF = tetrabutylammonium fluoride, DMP = Dess–Martin periodinane, EDCI = *N*-(3-dimethylaminopropyl)-*N*′-ethylcarbodiimide hydrochloride.

most unique types of NPs are easily overlooked by synthetic chemists and pharmacologists because of low activity in an insufficient number of pharmacological models. Thus, unique NPs can easily remain unexploited because the potential of the NP backbone has not been fully tapped. Previous strategies are not applicable to address this problem, due to mostly resulting in the natural-like scaffold. Here, we describe a 'pharmacophore-oriented semisynthesis' (POSS) approach to closely integrate natural scaffolds into biological research.

The pharmacophore-oriented semisynthesis approach was applied to create a novel anti-SARS-CoV-2 family by combining the pharmacophore of oridonin with a novel scaffold (maoelactone A, **1**). We first established **1** as a rearranged *ent*-kaurane diterpenoid with an unprecedented 1,10-*seco*-2,10-*abeo*-1,20-lactone scaffold from *Isodon erio-*

a

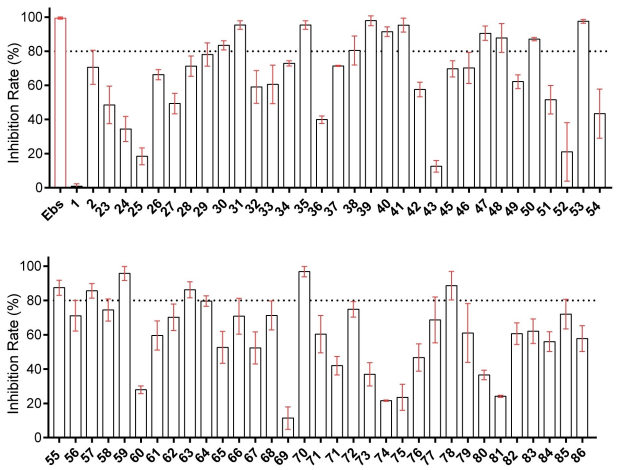

b

Compounds	IC_{50} (μM)	Compounds	IC_{50} (μM)
30	1.794 ± 0.099	**50**	1.662 ± 0.200
31	1.253 ± 0.158	**53**	0.523 ± 0.093
35	0.463 ± 0.013	**55**	1.115 ± 0.001
39	1.128 ± 0.322	**57**	2.427 ± 0.065
40	1.932 ± 0.146	**59**	1.731 ± 0.197
41	1.535 ± 0.310	**63**	2.304 ± 0.457
47	0.477 ± 0.012	**70**	0.824 ± 0.121
48	1.498 ± 0.144	**78**	1.093 ± 0.021

c

Compounds	SARS-CoV-2 affected Vero E6 cells			SARS-CoV-2 affected HPA EpiC cells		
	EC_{50} (μM)	CC_{50} (μM)	TI Value	EC_{50} (μM)	CC_{50} (μM)	TI Value
Remdesivir	0.04 ± 0.02	>200	>3333	0.196 ± 0.26	>200	>438.59
2	1.95 ± 0.59	24.24 ± 5.99	8.42~13.59	0.53 ± 0.14	14.18 ± 1.51	23.41~40.23
31	2.13 ± 3.02	21.59 ± 0.81	4.92~173.14	0.28 ± 0.23	>50	>98.03
35	0.98 ± 1.34	22.03 ± 0.89	11.04~566.	0.07 ± 0.06	15.91 ± 5.02	69.81~157.37
39	0.11 ± 0.02	4.29 ± 0.35	33.61~45.4	7.78 ± 2.38	20.30 ± 4.43	1.69~4.89
47	2.07 ± 2.52	3.95 ± 0.37	0.95~14.57	0.158 ± 0.156	15.84 ± 7.02	7.93~672.35
53	0.22 ± 0.26	17.13 ± 7.76	28.42~753.96	0.48 ± 0.23	>50	>67.67
55	0.020 ± 0.007	13.66 ± 0.56	523.81~555.41	0.18 ± 0.06	>50	>217.39
70	0.18 ± 0.23	>50	128.97~4859.23	0.019 ± 0.001	21.08 ± 0.99	>1000
78	0.54 ± 0.51	16.72 ± 5.67	23.02~71.83	2.88 ± 0.18	10.68 ± 2.43	2.69~4.85

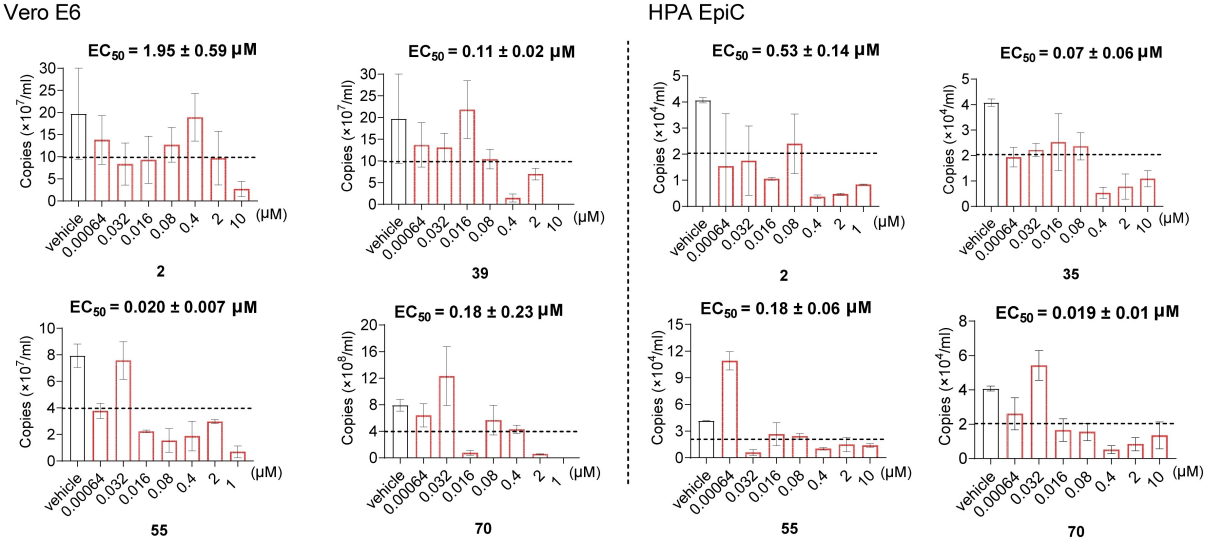

Figure 2. Discovery of SARS-CoV-2 $3CL^{Pro}$ inhibitors and anti-SARS-CoV-2 agents from the novel scaffold family. a) Inhibition rates of SARS-CoV-2 $3CL^{pro}$ with **23**–**86** at a concentration of 5 μM (Ebs = known inhibitor ebselen). b) IC_{50} value of selected compounds against SARS-CoV-2 $3CL^{pro}$. c) Antiviral activity of eight compounds against SARS-CoV-2 in cell-based assays comparing with remdesivir and **2**. Data are means ± SD; $n = 2$ biological replicates.

calyx and named the scaffold as maoelactone-type. We performed a ten-step semisynthesis of **1** from eriocalyxin B (**3**), providing the absolute configuration of a maoelactone-type scaffold. More importantly, the synthesis consisted of using a Wolff rearrangement/lactonization cascade (WRLC) to construct a maoelactone-type scaffold in one step, which played a key role in the implementation of the POSS approach. Further mechanistic study of the WRLC reaction suggests a concerted mechanism for Wolff rearrangement and a water-assisted stepwise process for lactonization. The developed WRLC reaction was then applied to transfer **2** into a maoelactone-type scaffold carrying the pharmacophore, which produced a novel scaffold family that was evaluated against SARS-CoV-2 $3CL^{Pro}$ and SARS-CoV-2. Batches of the members of the novel family showed significant anti-SARS-CoV-2 activity, of which **70** inhibited SARS-CoV-2 virus replication in HPA EpiC cells with a low EC_{50} value (19 ± 1 nM) and a high TI value (>1000), both values better than those of remdesivir.

Acknowledgements

We thank two anonymous reviewers for helpful suggestions, Prof. Zhi-Li Zuo for help with docking experiments, and Dr. Xiang Zhang for discussion. This project was supported financially by the NSFC-Joint Foundation of Yunnan Province (U2002221), the Second Tibetan Plateau Scientific Expedition and Research (STEP) program (2019QZKK0502), the National Natural Science Foundation of China (No. 81673329, 81874298, 22122104, 21933004 and 82151214), the CAS "Light of West China" Program, CAS Interdisciplinary Innovation Team (Pema-Tenzin Puno), the Yunnan Science Fund for Distinguished Young Scholars (2019FJ002), China Postdoctoral Science Foundation (2021M693237) and Yunnan Key Research and Development Program (202103AC100005).

Conflict of Interest

The authors declare no conflict of interest.

Data Availability Statement

The data that support the findings of this study are available in the Supporting Information of this article.

Keywords: Anti-SARS-CoV-2 Agents · Domino Reactions · Natural Products · Semisynthesis · Wolff Rearrangement

[1] a) P. Zhou, X.-L. Yang, X.-G. Wang, B. Hu, L. Zhang, W. Zhang, H.-R. Si, Y. Zhu, B. Li, C.-L. Huang, H.-D. Chen, J. Chen, Y. Luo, H. Guo, R.-D. Jiang, M.-Q. Liu, Y. Chen, X.-R. Shen, X. Wang, X.-S. Zheng, K. Zhao, Q.-J. Chen, F. Deng, L.-L. Liu, B. Yan, F.-X. Zhan, Y.-Y. Wang, G.-F. Xiao, Z.-L. Shi, *Nature* **2020**, *579*, 270–273; b) F. Wu, S. Zhao, B. Yu, Y.-M. Chen, W. Wang, Z.-G. Song, Y. Hu, Z.-W. Tao, J.-H. Tian, Y.-Y. Pei, M.-L. Yuan, Y.-L. Zhang, F.-H. Dai, Y. Liu, Q.-M. Wang, J.-J. Zheng, L. Xu, E. C. Holmes, Y.-Z. Zhang, *Nature* **2020**, *579*, 265–269.

[2] a) S. Ullrich, C. Nitsche, *Bioorg. Med. Chem. Lett.* **2020**, *30*, 127377; b) R. Hilgenfeld, *FEBS J.* **2014**, *281*, 4085–4096.

[3] a) M. Cully, *Nat. Rev. Drug Discovery* **2022**, *21*, 3–5; b) E. Mahase, *BMJ* **2021**, *375*, n2374; c) D. R. Owen, C. M. N. Allerton, A. S. Anderson, L. Aschenbrenner, M. Avery, S. Berritt, B. Boras, R. D. Cardin, A. Carlo, K. J. Coffman, A. Dantonio, L. Di, H. Eng, R. Ferre, K. S. Gajiwala, S. A. Gibson, S. E. Greasley, B. L. Hurst, E. P. Kadar, A. S. Kalgutkar, J. C. Lee, J. Lee, W. Liu, S. W. Mason, S. Noell, J. J. Novak, R. S. Obach, K. Ogilvie, N. C. Patel, M. Pettersson, D. K. Rai, M. R. Reese, M. F. Sammons, J. G. Sathish, R. S. P. Singh, C. M. Steppan, A. E. Stewart, J. B. Tuttle, L. Updyke, P. R. Verhoest, L. Wei, Q. Yang, Y. Zhu, *Science* **2021**, *374*, 1586–1593.

[4] Z. Jin, X. Du, Y. Xu, Y. Deng, M. Liu, Y. Zhao, B. Zhang, X. Li, L. Zhang, C. Peng, Y. Duan, J. Yu, L. Wang, K. Yang, F. Liu, R. Jiang, X. Yang, T. You, X. Liu, X. Yang, F. Bai, H. Liu, X. Liu, L. W. Guddat, W. Xu, G. Xiao, C. Qin, Z. Shi, H. Jiang, Z. Rao, H. Yang, *Nature* **2020**, *582*, 289–293.

[5] a) L. Zhang, D. Lin, X. Sun, U. Curth, C. Drosten, L. Sauerhering, S. Becker, K. Rox, R. Hilgenfeld, *Science* **2020**, *368*, 409–412; b) J. Qiao, Y.-S. Li, R. Zeng, F.-L. Liu, R.-H. Luo, C. Huang, Y.-F. Wang, J. Zhang, B. Quan, C. Shen, X. Mao, X. Liu, W. Sun, W. Yang, X. Ni, K. Wang, L. Xu, Z.-L. Duan, Q.-C. Zou, H.-L. Zhang, W. Qu, Y.-H.-P. Long, M.-H. Li, R.-C. Yang, X. Liu, J. You, Y. Zhou, R. Yao, W.-P. Li, J.-M. Liu, P. Chen, Y. Liu, G.-F. Lin, X. Yang, J. Zou, L. Li, Y. Hu, G.-W. Lu, W.-M. Li, Y.-Q. Wei, Y.-T. Zheng, J. Lei, S. Yang, *Science* **2021**, *371*, 1374–1378.

[6] W. Dai, B. Zhang, X.-M. Jiang, H. Su, J. Li, Y. Zhao, X. Xie, Z. Jin, J. Peng, F. Liu, C. Li, Y. Li, F. Bai, H. Wang, X. Cheng, X. Cen, S. Hu, X. Yang, J. Wang, X. Liu, G. Xiao, H. Jiang, Z. Rao, L.-K. Zhang, Y. Xu, H. Yang, H. Liu, *Science* **2020**, *368*, 1331–1335.

[7] J. Karges, M. Kalaj, M. Gembicky, S. M. Cohen, *Angew. Chem. Int. Ed.* **2021**, *60*, 10716–10723; *Angew. Chem.* **2021**, *133*, 10811–10818.

[8] a) N. J. Truax, D. Romo, *Nat. Prod. Rep.* **2020**, *37*, 1436–1453; b) S. Wang, G. Dong, C. Sheng, *Chem. Rev.* **2019**, *119*, 4180–4220; c) P. A. Wender, *Nat. Prod. Rep.* **2014**, *31*, 433–440; d) S. Wetzel, R. S. Bon, K. Kumar, H. Waldmann, *Angew. Chem. Int. Ed.* **2011**, *50*, 10800–10826; *Angew. Chem.* **2011**, *123*, 10990–11018; e) S. L. Schreiber, *Science* **2000**, *287*, 1964–1969; f) M. D. Burke, S. L. Schreiber, *Angew. Chem. Int. Ed.* **2004**, *43*, 46–58; *Angew. Chem.* **2004**, *116*, 48–60; g) R. W. Huigens III, K. C. Morrison, R. W. Hicklin, T. A. Flood, Jr., M. F. Richter, P. J. Hergenrother, *Nat. Chem.* **2013**, *5*, 195–202; h) Z. A. Könst, A. R. Szklarski, S. Pellegrino, S. E. Michalak, M. Meyer, C. Zanette, R. Cencic, S. Nam, V. K. Voora, D. A. Horne, J. Pelletier, D. L. Mobley, G. Yusupova, M. Yusupov, C. D. Vanderwal, *Nat. Chem.* **2017**, *9*, 1140–1149; i) M. E. Abbasov, R. Alvarino, C. M. Chaheine, E. Alonso, J. A. Sanchez, M. L. Conner, A. Alfonso, M. Jaspars, L. M. Botana, D. Romo, *Nat. Chem.* **2019**, *11*, 342–350.

[9] E. Fujita, T. Fujita, H. Katayama, M. Shibuya, *Chem. Commun.* **1967**, 252–254.

[10] a) Y. Ding, D. Li, C. Ding, P. Wang, Z. Liu, E. A. Wold, N. Ye, H. Chen, M. A. White, Q. Shen, J. Zhou, *J. Med. Chem.* **2018**, *61*, 2737–2752; b) Y. Ding, C. Ding, N. Ye, Z. Liu, E. A. Wold, H. Chen, C. Wild, Q. Shen, J. Zhou, *Eur. J. Med. Chem.* **2016**, *122*, 102–117.

[11] Z.-R. Zhang, Y.-N. Zhang, X.-D. Li, H.-Q. Zhang, S.-Q. Xiao, F. Deng, Z.-M. Yuan, H.-Q. Ye, B. Zhang, *Signal Transduction Targeted Ther.* **2020**, *5*, 218.
[12] a) D. R. Littler, M. Liu, J. L. McAuley, S. A. Lowery, P. T. Illing, B. S. Gully, A. W. Purcell, I. R. Chandrashekaran, S. Perlman, D. F. J. Purcell, R. J. Quinn, J. Rossjohn, *J. Biol. Chem.* **2021**, *297*, 101362; b) B. Zhong, W. Peng, S. Du, B. Chen, Y. Feng, X. Hu, Q. Lai, S. Liu, Z.-W. Zhou, P. Fang, Y. Wu, F. Gao, H. Zhou, L. Sun, *Small Sci.* **2022**, *0*, 2100124.
[13] a) C. Ding, Y. Zhang, H. Chen, Z. Yang, C. Wild, L. Chu, H. Liu, Q. Shen, J. Zhou, *J. Med. Chem.* **2013**, *56*, 5048–5058; b) C. Ding, Y. Zhang, H. Chen, C. Wild, T. Wang, M. A. White, Q. Shen, J. Zhou, *Org. Lett.* **2013**, *15*, 3718–3721; c) C. Ding, Y. Zhang, H. Chen, Z. Yang, C. Wild, N. Ye, C. D. Ester, A. Xiong, M. A. White, Q. Shen, J. Zhou, *J. Med. Chem.* **2013**, *56*, 8814–8825.
[14] P.-Q. Shen, H.-D. Sun, *Acta Bot. Yunnanica* **1986**, *8*, 163–166.
[15] a) K. Chávez, R. S. Compagnone, A. Álvarez, K. Figarella, I. Galindo-Castro, S. Marsiccobetre, J. Triviño, I. Arocha, A. Taddei, G. Orsini, S. Tillett, A. I. Suárez, *Bioorg. Med. Chem.* **2015**, *23*, 3687–3695; b) Y. Zhao, X.-M. Niu, L.-P. Qian, Z.-Y. Liu, Q.-S. Zhao, H.-D. Sun, *Eur. J. Med. Chem.* **2007**, *42*, 494–502.
[16] Deposition Numbers 2078764 (for **11**), 2078763 (for **13**), 2078766 (for **18**) and 2078765 (for **S3**) contains the supplementary crystallographic data for this paper. These data are provided free of charge by the joint Cambridge Crystallographic Data Centre and Fachinformationszentrum Karlsruhe Access Structures service.
[17] P. A. Jacobi, K. Lee, *J. Am. Chem. Soc.* **2000**, *122*, 4295–4303.
[18] Y. Xia, Y. Liang, Y. Chen, M. Wang, L. Jiao, F. Huang, S. Liu, Y. Li, Z.-X. Yu, *J. Am. Chem. Soc.* **2007**, *129*, 3470–3471.
[19] Q. Xiao, W.-W. Ren, Z.-X. Chen, T.-W. Sun, Y. Li, Q.-D. Ye, J.-X. Gong, F.-K. Meng, L. You, Y.-F. Liu, M.-Z. Zhao, L.-M. Xu, Z.-H. Shan, Y. Shi, Y.-F. Tang, J.-H. Chen, Z. Yang, *Angew. Chem. Int. Ed.* **2011**, *50*, 7373–7377; *Angew. Chem.* **2011**, *123*, 7511–7515.
[20] M. A. Baker, R. M. Demoret, M. Ohtawa, R. A. Shenvi, *Nature* **2019**, *575*, 643–646.
[21] S. M. Kissler, C. Tedijanto, E. Goldstein, Y. H. Grad, M. Lipsitch, *Science* **2020**, *368*, 860–868.
[22] a) H.-D. Sun, S.-X. Huang, Q.-B. Han, *Nat. Prod. Rep.* **2006**, *23*, 673–698; b) M. Liu, W.-G. Wang, H.-D. Sun, J.-X. Pu, *Nat. Prod. Rep.* **2017**, *34*, 1090–1140.
[23] a) F. Peng, S. J. Danishefsky, *J. Am. Chem. Soc.* **2012**, *134*, 18860–18867; b) P. Lu, A. Mailyan, Z. Gu, D. M. Guptill, H. Wang, H. M. L. Davies, A. Zakarian, *J. Am. Chem. Soc.* **2014**, *136*, 17738–17749; c) C. Zheng, I. Dubovyk, K. E. Lazarski, R. J. Thomson, *J. Am. Chem. Soc.* **2014**, *136*, 17750–17756; d) A. Cernijenko, R. Risgaard, P. S. Baran, *J. Am. Chem. Soc.* **2016**, *138*, 9425–9428.
[24] J. Wu, Y. Kadonaga, B. Hong, J. Wang, X. Lei, *Angew. Chem. Int. Ed.* **2019**, *58*, 10879–10883; *Angew. Chem.* **2019**, *131*, 10995–10999.
[25] a) B. Hong, W. Liu, J. Wang, J. Wu, Y. Kadonaga, P.-J. Cai, H.-X. Lou, Z.-X. Yu, H. Li, X. Lei, *Chem* **2019**, *5*, 1671–1681; b) W. Liu, H. Li, P.-J. Cai, Z. Wang, Z.-X. Yu, X. Lei, *Angew. Chem. Int. Ed.* **2016**, *55*, 3112–3116; *Angew. Chem.* **2016**, *128*, 3164–3168.
[26] J. Guo, B. Li, W. Ma, M. Pitchakuntla, Y. Jia, *Angew. Chem. Int. Ed.* **2020**, *59*, 15195–15198; *Angew. Chem.* **2020**, *132*, 15307–15310.
[27] Y. Que, H. Shao, H. He, S. Gao, *Angew. Chem. Int. Ed.* **2020**, *59*, 7444–7449; *Angew. Chem.* **2020**, *132*, 7514–7519.
[28] B. Wang, Z. Liu, Z. Tong, B. Gao, H. Ding, *Angew. Chem. Int. Ed.* **2021**, *60*, 14892–14896; *Angew. Chem.* **2021**, *133*, 15018–15022.

Manuscript received: January 30, 2022
Accepted manuscript online: April 28, 2022
Version of record online: May 12, 2022